Control of Water Adsorption via Electrically Doped Graphene

*Morteza H. Bagheri,† Rebecca T. Loibl,† Scott N. Schiffres†‡**

† Department of Mechanical Engineering, Binghamton University, State University of New York, Binghamton, NY 13902, USA

‡ Materials Science and Engineering Program, Binghamton University, State University of New York, Binghamton, NY 13902, USA

*Corresponding Author: sschiffr@binghamton.edu

Keywords: water adsorption, doped graphene, tunable adsorption, tunable wettability.

The interaction of graphene with water molecules under an applied electric field is not thoroughly understood, yet this interaction is important to many thermal, fluidic, and electrical applications of graphene. In this work, the effect of electrical doping of graphene on water adsorption was studied through adsorption isotherms and current-voltage (IV) characterizations as a function of the Fermi level. The water adsorption onto graphene increased ~15% and the doping levels increased by a factor of three with a gate-to-graphene voltage of +20 or –20V compared to 0V for sub-monolayer adsorption. This change in uptake is attributed to the increase in density of state of graphene upon electrical-doping, which changes the Coulombic and van der Waals interactions. The water adsorption onto graphene is either *n*- or *p*-doping depending on the applied gate-to-graphene voltage. The ambi-doping nature of water onto graphene is due to the polar nature of water molecules, so the doping depends on the orientation of the water molecules.

1. Introduction

Water condensation onto a surface begins with the adsorption of water vapor. This is followed by the creation of hydrogen bonds among water molecules, which coalesce to form droplets. Adsorption plays an important role in applications such as condensation-evaporation in thermal power generation,[1,2] ambient air water harvesting,[3,4] ice-nucleation,[5] self-cleaning surfaces,[6,7] and oil-water separation[8,9] The energy efficiency of these adsorption technologies can be improved by tunable adsorption.[10,11] For example, in condensation heat transfer, tunable adsorption could enable a surface to condense more vapor by periodically switching between being easier to form a condensation film to easier to shed condensation. However, no method to reversibly control water adsorption has been detailed in the literature.

Being extremely thin and thermally stable, graphene is an appealing method of surface modification.[12,13] For instance, the contact angle of water on graphene has been found to be controllable through electrical- and chemical-doping.[14,15] However, there is a lack of experimental investigation relating to adsorption on graphene. It has been noted that water adsorption onto a supported graphene changes graphene's electronic structure. Density functional theory (DFT) calculations have shown water adsorption tunes the charge carrier concentration and shifts the Fermi level of graphene in the case of weak physical contact between graphene and the supporting substrate (such as Cu, Pt, Au, Al, and Ag),.[16,17] Moreover, studies have incidentally demonstrated that chemisorption of oxygen onto bilayer graphene can be altered by changing the gate-graphene voltage.[18] However, how water adsorption changes with altering the graphene Fermi level has never been studied experimentally.

Therefore, we set out to test the hypothesis that the water adsorption behavior onto graphene can be tuned by electrically shifting the Fermi level, and hence the energetics of adsorption. In order

to test this hypothesis, water adsorption onto back-gated graphene field effect transistors (GFETs) was studied as a function of electrical-doping via a quartz crystal microbalance (QCM) and current-voltage (IV) curve measurements.

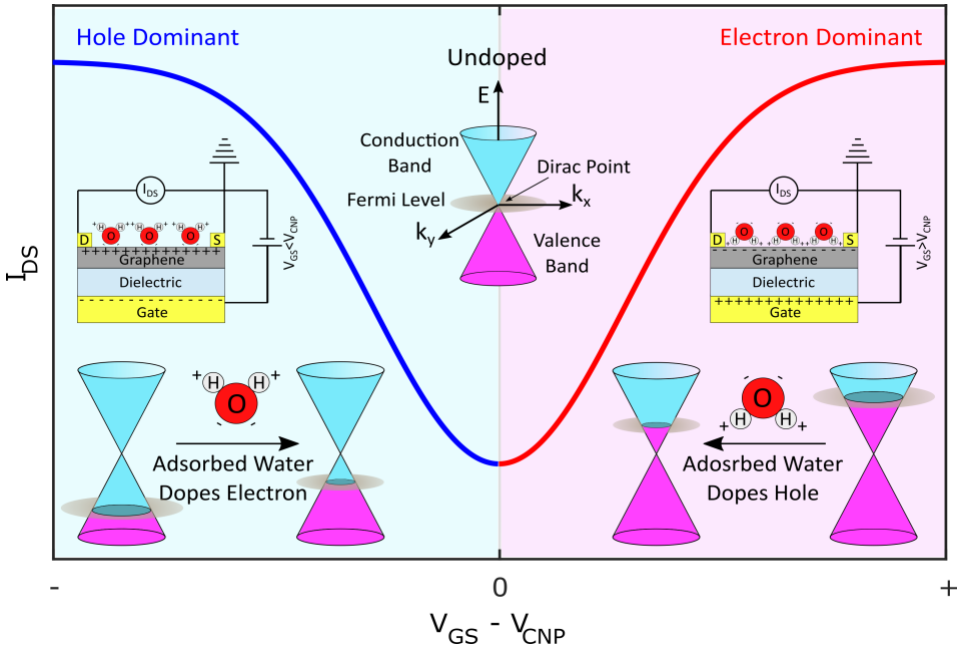

Figure 1 An illustration of how the gate voltage is hypothesized to modify the energetics and orientation of water adsorption in a back-gate GFET. (left) When the gate-graphene voltage is less than the charge neutral point, $V_{GS} - V_{CNP} < 0$, the Fermi level shifts down, electrically *p*-doping the graphene. This should make adsorption that chemically *n*-dopes graphene favored, which leads to water molecules adsorbing with the OH legs upward. (right) Inversely, when $V_{GS} - V_{CNP} > 0$, the Fermi level shifts up, electrically *n*-doping the graphene. This thereby should make adsorption that chemically *p*-dopes graphene favored, like water molecules adsorbing with the OH legs downward.

2.Results and Discussion

GFET IV curves illustrate the current through a graphene channel as function of the gate-graphene voltage (**Figure 1**). The gate-graphene voltage (V_{GS}) with the minimum conductance represents the charge neutral point (V_{CNP}). A pristine (undoped) graphene has its minimum conductance at zero-gate voltage, where its mobility is maximum and the carrier density is minimum (the Dirac

Point).[19] For $V_{GS} - V_{CNP} > 0$, the Fermi level shifts upward, and *n*-dopes graphene. Conversely, when $V_{GS} - V_{CNP} < 0$, the applied electric field extracts electrons from the valence band to create holes, which results in shifting the Fermi level downward, *p*-doping the graphene.

To measure the mass of adsorbed water vs the applied gate voltage, i.e., as a function of shifting the Fermi level, the GFETs were fabricated on QCMs (**Figure S1**). Adsorption isotherms were measured in an environmental vacuum chamber (**Figure S2**) using the shift in the resonance frequency of the QCM upon water vapor exposure. In a temperature-controlled environment, the resonance frequency of a QCM depends on the magnitude of the adsorbed mass, the effect of the hydrostatic pressure on the elastic modulus of quartz, and the viscoelastic coupling to the gas.[20,21] Corrections for pressure and viscoelastic coupling were made to calculate the mass adsorbed.[22] **Figure 2**a shows the adsorption isotherms of water onto graphene for three different gate voltages: 0V, +20V, and –20V. In these experiments, graphene was exposed to water vapor while the gate voltage was held constant. Before each adsorption experiment, the sample was annealed to initialize the graphene back to nearly identical IV curves and V_{CNP} (**Figure 2**b). The repeatability of the isotherms for the monolayer region on the same sample are shown in **Figure S3**a. The uptake versus gate voltage from a second GFET is shown in **Figure S3**b and indicates a similar trend, though the amplitude is slightly different due to slight differences in the size of the graphene channel and sample-to-sample variation.

The three applied gate voltages during water adsorption, 0V, +20V, and –20V, induced no doping, *n*-doping, and *p*-doping, respectively. It can be seen in Figure 2a that the non-zero-gate voltages led to higher uptakes. However, switching the gate voltage polarity resulted in similar uptakes. For example, at ~3 Torr where we expected approximately a monolayer of adsorbed water,[23] the uptake was ~15% higher at gate voltages of +20V and –20V than at 0V.. DFT calculations have

shown higher adsorption energy of gases, including water vapor, on doped graphene compared to undoped graphene,[14,15] where according to the Langmuir model, the higher adsorption energy should result in higher adsorption uptake.[24] This change in uptake for the doped graphene is attributed to the change in the Coulombic and van der Waals interactions due to the increase in density of state (DOS) of graphene upon doping.[14]

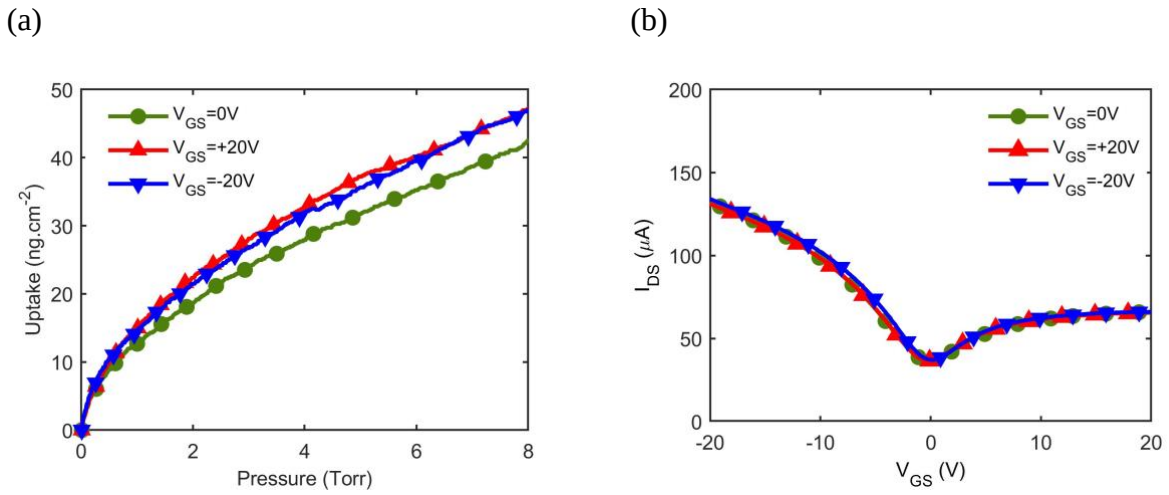

Figure 2 (a) Adsorption isotherms of water onto graphene at three different gate voltages: 0V, +20V, –20V. The isotherms show higher uptakes for non-zero-gate voltages than zero-gate voltage. (b) The corresponding IV curves prior to each test while under high vacuum. The IV curves prior to water adsorption show no hysteresis after annealing.

To gain insight into the doping of graphene due to water adsorption under an applied electric field, an additional set of experiments measured the electronic properties of graphene during adsorption. In these experiments, the gate voltage was kept at a constant value (+20V, –20V, or 0V), while IV scans were periodically conducted after x minutes of water vapor exposure (x = 0, 1, 2, …, 20). To avoid further adsorption/desorption during IV scans, the chamber was evacuated for 1 min prior to each scan (maximum pressure of 5 mTorr). The gate voltage during IV scans started and ended at the adsorption gate voltage. For the adsorption tests with an applied +20V gate, the IV gate voltage was swept from +20V to –20V and then back to +20V. Conversely, for the –20V

adsorption test, the gate voltage was swept from –20V to +20V, then back to –20V. Adsorption tests were performed for the zero-gate voltage with both sweep procedures (+20V→–20V→+20V and –20V→+20V→–20V). The purpose of running two adsorption tests at zero-gate voltage was to see how the sweep direction affects water adsorption onto graphene and if the graphene-water interface remembers the last applied gate voltage. For all measurements, the drain-source voltage was kept at 0.1V, which is in the ohmic region.

Figure 3 shows the IV curves after water vapor exposure with different applied gate voltages. During the adsorption with an applied gate voltage of +20V, the graphene was initially *n*-doped due to the applied gate voltage; however, the adsorption of water molecules shifted the V_{CNP} in the positive direction and made the graphene less *n*-doped (Figure 3a), i.e., water adsorption induced holes in graphene. On the other hand, when the applied gate voltage was kept at –20V during adsorption, the graphene was initially *p*-doped due to the applied gate voltage; however, the adsorption of water molecules moved the V_{CNP} in the negative direction and made the graphene less *p*-doped (Figure 3b), i.e., water adsorption induced electrons in graphene. Figure 3c and Figure 3d show the IV curves after water vapor exposure while the gate voltage was kept at 0V during adsorption. In Figure 3c the sweeps started and ended at +20V and in Figure 3d they started and ended at –20V.

Figure 4 shows the voltage driving electrical doping, the shift in the V_{CNP}, the induced doping, and the shift in the Fermi level versus water vapor exposure time. For these calculations, the IV curves were fit to an asymmetric Lorentzian.[25] The shift in the Fermi level was calculated based on:

$$\Delta E_F(t) = -\Delta n(t)/|\Delta n(t)| \,.\, \hbar v_f \sqrt{\pi |\Delta n(t)|} \qquad (1)$$

where $\hbar$ and ν_f are the reduced Planck's constant and the Fermi velocity of graphene, respectively.[26,27] The doping induced by the molecular adsorption at time t, Δn(t), is equal to:

$$\Delta n(t) = (c_g/e)[V_{CNP}(t) - V_{CNP}(0)] \quad (2)$$

where c_g is the gate capacitance per unit area (C_g/A), e is the elementary charge, and $V_{CNP}(t)$ represent the charge neutral point voltage at time t.[18]

It is observed that a larger applied gate voltage during water adsorption results in higher doping density, Δn, which is proportional to the water uptake (Figure 4c). Nonetheless, the polarity of the gate does not significantly change the amount of adsorbed water, but it does affect the carrier type. This observation demonstrates that electrically doping graphene can result in more hydrophilic surfaces. Moreover, an applied gate voltage at V_{CNP} will make the graphene as hydrophobic as possible. This agrees with the numerical and experimental contact angle measurements of water on electrically doped graphene, where an undoped graphene results in greater water contact angle.[14,28]

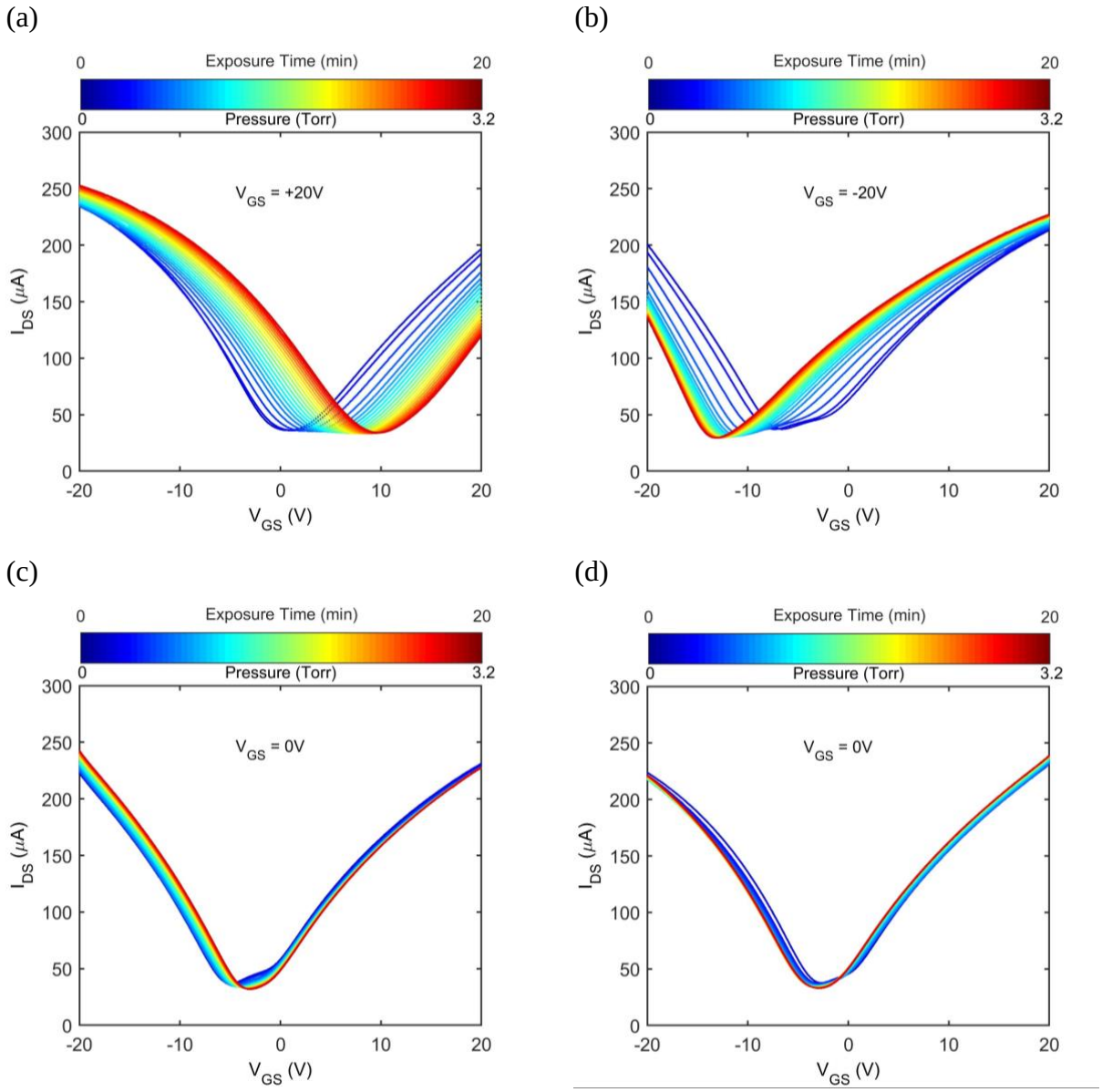

Figure 3 IV curves measured under vacuum after *x* minutes (*x* = 0, 1, 2, …, 20) of water vapor exposure with the gate voltage at (a) +20V, (b) –20V, and (c, d) 0V. The gate voltage sweep in (a) and (c) was +20V →–20V →+20V, and in (b) and (d) was –20V →+20V →–20V. The chemical doping due to adsorption of water vapor is larger for the +20V and –20V tests (panels a, b) than the 0V tests (panels c, d), as indicated by their greater shift of their charge neutral. It is also noted that the direction of the charge neutral point shift is opposite for the +20V and –20V tests (panels a,b), demonstrating that water can ambi-dope graphene. The 0V tests also demonstrate small and opposite shifts in the change neutral point due to hysteresis from the vacuum applied gate sweep voltage.

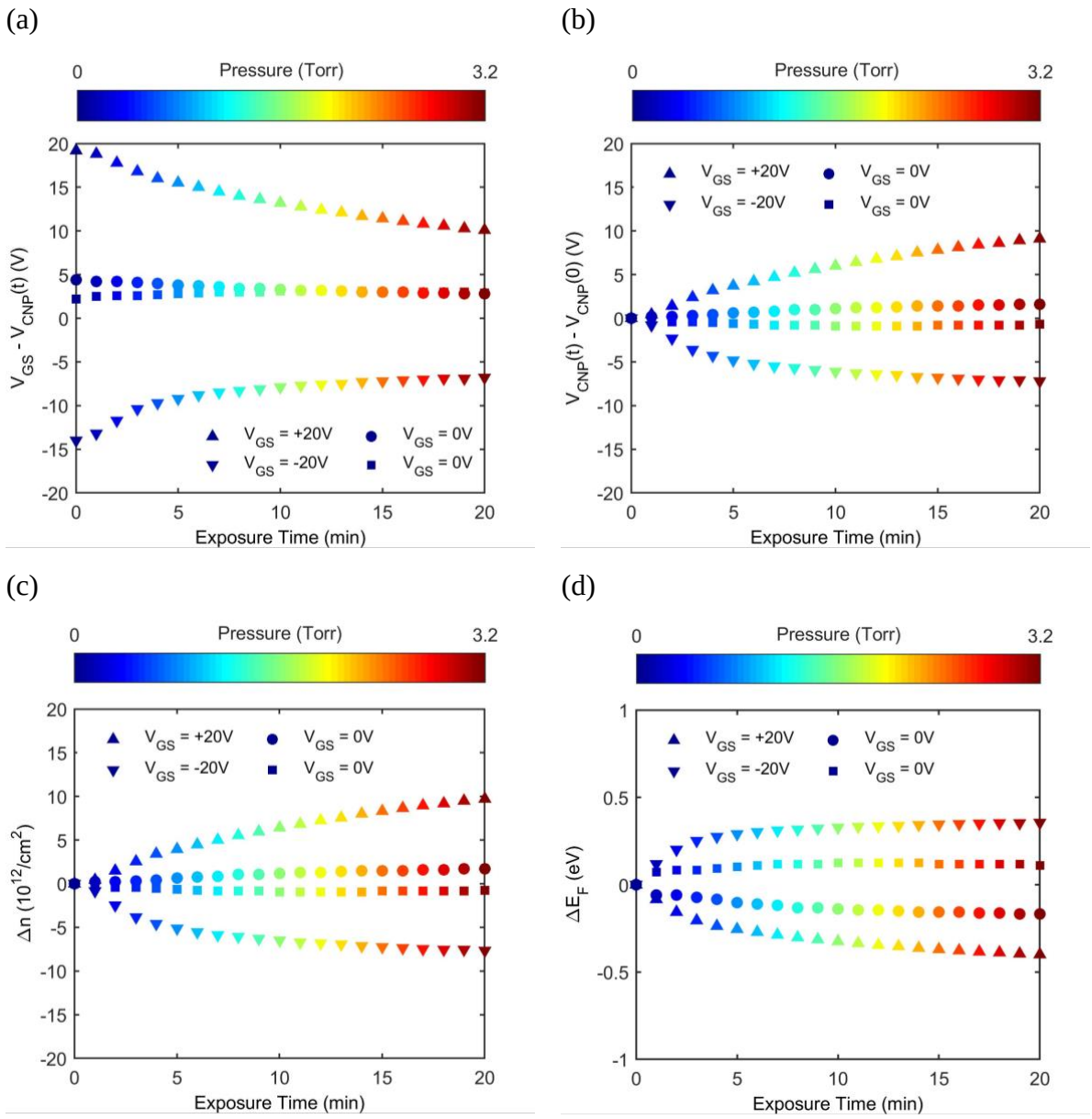

Figure 4 (a) The difference between the applied gate voltage and the charge neutral point versus water vapor exposure time for gate voltages of +20V (△), –20V (▽), 0V (○), and 0V (□). (b) The shift of the V_{CNP} upon water exposure at the different gate voltages. (c,d) The corresponding doping density (c) and the shift of the Fermi level due to water adsorption (d). The IV curves were measured under vacuum. The IV gate-graphene voltage was swept +20V →–20V →+20V for △ and ○ measurements, and swept –20V →+20V →–20V for ▽ and □ measurements. The doping densities and Fermi level shifts were greater for the +20V and –20V tests than those at 0V. The chemical doping due to adsorption was opposite for the +20V and –20V tests. The doping difference between the two 0V tests was due to hysteresis from the gate sweep.

Many dopants fall clearly into one of these two categories: electron-donor molecules that *n*-dope graphene and electron-acceptor molecules that *p*-dope;[18,29] however, the doping induced by water adsorption onto graphene depends on the orientation of the adsorbed water molecule, which is controlled by the electric field at the supporting substrate.[16,30] The higher electronegativity of oxygen compared to hydrogen in water molecules creates an electrical dipole moment with partial negative charge on the oxygen atom and partial positive charges on the hydrogen atoms. This dipole moment in water molecules affects its adsorption onto graphene.[12,14,27]

Depending on the orientation of the adsorbed water molecule, it can either *p*-dope or *n*-dope graphene. In a water molecule, the HOMO (Highest Occupied Molecular Orbital) is completely located on the O atom and the LUMO (Lowest Unoccupied Molecular Orbital) is mostly located on the H atoms. Due to the relative positions of the HOMO and the LUMO of a water molecule with respect to the Dirac point, if the O atom points to graphene (O-H bond pointing up), the HOMO plays the dominant role and donates charge from water to graphene through a small mixing with graphene orbitals above the Fermi level, inducing *n*-doping. If the H atoms point to graphene (O-H bond pointing down), there is a small charge transfer from graphene to the water molecule through a small mixing with the graphene orbitals below the Dirac point that induces *p*-doping.[29]

When the applied gate voltage is greater than the V_{CNP} ($V_{GS} > V_{CNP}$) the graphene is *n*-doped and electrons are the dominant charge carriers in graphene, so that water molecules tend to adsorb onto graphene with the positive side of the dipole (H atoms towards graphene), which induces *p*-doping (**Figure 1**). Figure 3a supports this hypothesis, as when V_{GS} was greater than V_{CNP} (V_{GS} = +20V), the V_{CNP} shifted in the positive direction, which indicates water is *p*-doping graphene. Conversely, when the gate voltage is less than the V_{CNP}, the water molecules adsorb onto graphene with the OH bonds upward, which *n*-dopes graphene (**Figure 1**). This agrees with Figure 3b, where V_{GS} was

less than V_{CNP} (V_{GS} = –20V), and the V_{CNP} shifted in the negative direction, which indicates water is *n*-doping graphene.

In the two adsorption tests where the gate voltage was held at zero during water exposure, there was hysteresis due to the last gate voltage applied during the vacuum IV measurements. This is thought to be due to adsorbed water molecules aligning according to the last applied gate voltage. For these zero-gate water exposure tests, the adsorption induced doping polarity was controlled by the last gate voltage of the vacuum IV scan. In the zero-gate water exposure test with IV sweeps starting and ending at a gate voltage of +20V, the water molecules adsorbed with the OH bonds downward, which resulted in *p*-doping graphene. In the other zero-gate voltage test where the voltage sweep started and ended at a gate of –20V, water molecules adsorbed with the oxygen pointing towards the graphene, hence *n*-doping. The larger shift of the V_{CNP} during the tests with non-zero-gate voltages shows that an applied gate voltage can enhance the water adsorption onto graphene; however, due to the dipole nature of the water molecules, the polarity of the gate did not noticeably affect adsorption uptake.

We showed that electrically doping graphene enhances the water uptake onto graphene; however, we were also interested to see whether electrically doping graphene accelerates water adsorption kinetics. We calculated the doping rates by numerically differentiating the doping density with respect to time and pressure. Figure 5 captures the effect of a gate voltage on the kinetics of water adsorption onto graphene in terms of the doping vs time and doping vs pressure. When the gate voltage is larger in magnitude compared to V_{CNP}, i.e., a bigger $|V_{GS} – V_{CNP}|$, it results in faster adsorption of water onto graphene. This shows that when the Fermi level is further from the Dirac point (either direction), it is more likely for a water molecule to adsorb onto graphene. We suspect

this is due to the change in Fermi level leading to more energetic adsorption, a greater accommodation coefficient, and faster kinetics.

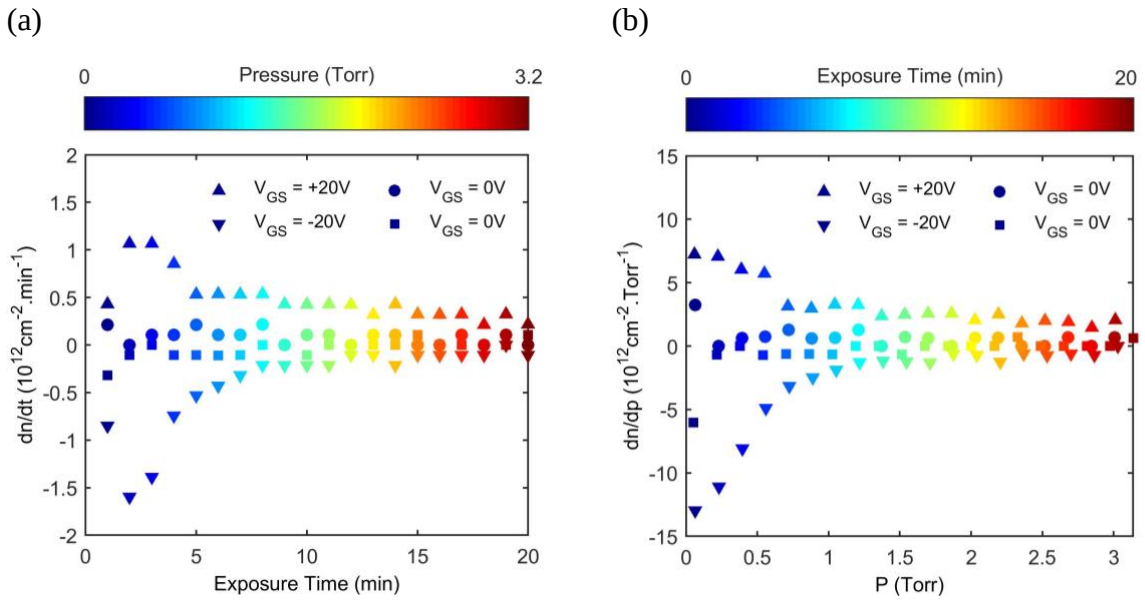

Figure 5 (a) The doping rate versus exposure time for different gate voltages. (b) The change in doping per change in water vapor pressure. Symbols for different gate voltages are the same as in Figure 4. The kinetics of adsorption are larger in magnitude for the +20V and –20V than the 0V tests.

3. Conclusion

The water adsorption onto electrically doped graphene was investigated using a back-gate GFET fabricated onto a QCM. IV curves were measured before and after water vapor exposure while the gate voltage was held at +20V, –20V, or 0V. The measured IV curves and isotherms showed that water adsorption onto graphene depends on the doping of graphene and increases with $|V_{GS}-V_{CNP}|$. Whether graphene is *n*- or *p*-doped due to water vapor adsorption depends on the polarity of the gate voltage. For electrically *n*-doped graphene, water molecules tend to adsorb onto graphene with the hydrogens facing graphene and move the Fermi level lower (*p*-doping). On the other hand, if the gate voltage induces *p*-doping, water molecules will adsorb with the oxygen facing graphene

and move the Fermi level higher (*n*-doping). The adsorption isotherms showed higher uptakes for electrically doped than non-electrically doped graphene. Not only do larger gate voltages increase the water adsorption, they accelerated the adsorption process as well. These findings could be used to tune the hydrophilicity/hydrophobicity of a surface. The conclusions are hypothesized to extend more widely to physisorption by polar molecules onto 2D field effect transistors.

4. Experimental Methods

4.1. Apparatus

An apparatus with the ability to measure the adsorption isotherms under different gases, and the electronic properties of 2D materials, was designed and constructed as shown in **Figure S2**. The environmental vacuum chamber was equipped with a custom QCM holder to measure IV curves (KEITHLEY SMU 2614B). A dry pumping station (PFEIFFER HiCube 80 Eco) that reaches a base pressure of $1x10^{-6}$ Torr (MKS 390 Micro-Ion® ATM) was used with a LN_2 trap. The chamber was temperature controlled via a recirculation bath (HAAKE K20, Glass Encapsulated Thermistors 55004). DI water (SIGMA-ALDRICH 38796) was degassed through multiple freeze-pump-thaw cycles and was used as the vapor source for water adsorption. A modified 5 MHz AT-cut QCM measured adsorption uptake (Stanford Research Systems QCM200, FilTech). Vapor pressure was measured using two heated capacitance manometers (Kurt J. Lesker HCG045-OT-1-1 and HCG045-FT-1-1). All the sensors were monitored via a data acquisition logger (KEITHLEY DAQ6510) using MATLAB.

4.2. Sample Preparation

Back-gate GFETs were fabricated onto 5MHz AT-cut QCMs (**Figure S1**). The top electrode of the QCM also served as the gate for the transistor. The QCM with Au electrodes was sonicated for

15 min in acetone, methanol, and isopropyl alcohol, respectively. As an adhesion layer, 100 nm of Ti was deposited onto the top electrode of the QCM via E-beam evaporation (AJA International). A 100 nm Al_2O_3 was deposited via atomic layer deposition (ALD) with trimethylaluminum (TMA) and oxygen plasma at 200 ºC (OXFORD Flex AL) to form the dielectric onto the QCM.

After the dielectric deposition, PMMA-backed CVD graphene (Graphenea Monolayer Graphene on Polymer Film) was transferred onto the QCM. The samples were dried in air for 30 min, followed by baking on a hotplate at 150 ºC for 1 hr. Then, the samples were kept under low vacuum (0.1 Torr) for 24 hrs to remove the trapped water between the substrate and graphene. To remove PMMA from the graphene, the samples were soaked in acetone at 50 ºC for 1 hr and then in isopropyl alcohol for another hour, followed by drying with N_2. To further remove PMMA trace residuals, the samples were annealed at 300 ºC and $1x10^{-8}$ Torr for 2 hrs with a ramping temperature of 5 ºC /min. Previously, we investigated the quality of graphene, transferred with the same process, via X-ray Photoelectron Spectroscopy (XPS) and found over 77% of the surface was covered by sp^2 bonded carbon .[22] After the graphene transfer, the drain and source (5 nm Cr / 100 nm Au) were deposited on top of graphene via E-beam evaporation (AJA International), creating a 7.1 mm × 7.1 mm channel that overlaps with the top electrode of the QCM. The dielectric capacitance was measured via KEITHLEY 4200-SCS. The entire fabrication process was conducted in a class 100 clean room. **Figure S4** and **Figure S5** show the Raman Spectroscopy and Atomic Force Microscopy (AFM) conducted on one of the samples, respectively. The D to G and 2D to G Raman peak ratios are 1:20 and 4:1, respectively, indicating low defect single layer graphene. The roughness was about 1.5nm was comparable to the substrate roughness.

Before each test, the sample was annealed *ex situ* at 150 ºC for 1 hr under high vacuum ($1x10^{-8}$ Torr). Then, it was transferred to the test chamber and pumped down for 18 hrs under high vacuum

($1x10^{-6}$ Torr) before each adsorption test. This procedure was done to help the graphene return to its initial V_{CNP}.

Supporting Information

Schematics of the experimental setup; An illustration of the sample preparation steps; The repeatability of the adsorption isotherms; Raman Spectroscopy and Atomic Force Microscopy of one sample.

Author Contributions

SNS conceived and supervised the project. MHB designed the experiments, fabricated the samples, conducted the experiments, and analyzed the data. RTL helped with experimental tool design. MHB wrote the manuscript in consultation with SNS and RTL.

Acknowledgements

We greatly appreciate the helpful conversations with Shawn Wagoner, Vincent Genova, Tara Dhakal, and Jeffrey Mativetsky. We also appreciate SUNY Binghamton's Transdisciplinary Area of Excellence Seed Grant. RTL acknowledges Scholarship Program for Master's Degree Seeking Students in Engineering (Grant No. NSF DUE-1458739). We also acknowledge the help of Julia Billman and the NSF REU Grant No. NSF DMR-1658990 with some of the tool development and Yingchun Jiang for her assistance in conducting AFM measurements. This work was performed in part at the Cornell NanoScale Facility, a member of the National Nanotechnology Coordinated Infrastructure (NNCI), which is supported by the National Science Foundation (Grant NNCI-2025233).

References

[1] N. Miljkovic, R. Enright, Y. Nam, K. Lopez, N. Dou, J. Sack, E. N. Wang, *Nano Lett.* **2013**, *13*, 179.

[2] J. Oh, R. Zhang, P. P. Shetty, J. A. Krogstad, P. V. Braun, N. Miljkovic, *Adv. Funct. Mater.* **2018**, *28*, 1707000.

[3] H. Kim, S. Yang, S. R. Rao, S. Narayanan, E. A. Kapustin, H. Furukawa, A. S. Umans, O. M. Yaghi, E. N. Wang, *Science* **2017**, *356*, 430.

[4] L. Zhong, H. Zhu, Y. Wu, Z. Guo, *J. Colloid Interface Sci.* **2018**, *525*, 234.

[5] C. Cline, **2019**.

[6] Y. C. Jung, B. Bhushan, *ACS Nano* **2009**, *3*, 4155.

[7] A. R. Bielinski, M. Boban, Y. He, E. Kazyak, D. H. Lee, C. Wang, A. Tuteja, N. P. Dasgupta, *ACS Nano* **2017**, *11*, 478.

[8] T. M. McCoy, S. A. Holt, A. M. Rozario, T. D. M. Bell, R. F. Tabor, *Adv. Mater. Interfaces* **2017**, *4*, 1700803.

[9] G. A. Turpin, S. A. Holt, J. M. P. Scofield, B. M. Teo, R. F. Tabor, *Adv. Mater. Interfaces* **2020**, *7*, 1901810.

[10] M. H. Bagheri, S. N. Schiffres, *Langmuir* **2018**, *34*, 1908.

[11] Y. Jiang, M. H. Bagheri, R. T. Loibl, S. N. Schiffres, *Appl. Therm. Eng.* **2019**, *160*, 113906.

[12] J. Rafiee, X. Mi, H. Gullapalli, A. V. Thomas, F. Yavari, Y. Shi, P. M. Ajayan, N. A. Koratkar, *Nat. Mater.* **2012**, *11*, 217.

[13] D. J. Preston, D. L. Mafra, N. Miljkovic, J. Kong, E. N. Wang, *Nano Lett.* **2015**, *15*, 2902.

[14] G. Hong, Y. Han, T. M. Schutzius, Y. Wang, Y. Pan, M. Hu, J. Jie, C. S. Sharma, U. Müller, D. Poulikakos, *Nano Lett.* **2016**, *16*, 4447.

[15] X.-Y. Liang, N. Ding, S.-P. Ng, C.-M. L. Wu, *Appl. Surf. Sci.* **2017**, *411*, 11.

[16] X. Li, J. Feng, E. Wang, S. Meng, J. Klimeš, A. Michaelides, *Phys. Rev. B* **2012**, *85*, 085425.

[17] S. Naghdi, G. Sanchez-Arriaga, K. Y. Rhee, *J. Alloys Compd.* **2019**, *805*, 1117.

[18] Y. Sato, K. Takai, T. Enoki, *Nano Lett.* **2011**, *11*, 3468.

[19] Y.-W. Tan, Y. Zhang, K. Bolotin, Y. Zhao, S. Adam, E. H. Hwang, S. Das Sarma, H. L. Stormer, P. Kim, *Phys. Rev. Lett.* **2007**, *99*, 246803.

[20] K. H. Behrndt, *Vacuum Microbalance Techniques: Volume 5*, Springer US, **1966**.

[21] L. Bruschi, G. Mistura, *Phys. Rev. B* **2001**, *63*, 235411.

[22] M. H. Bagheri, R. T. Loibl, J. A. Boscoboinik, S. N. Schiffres, *Carbon* **2019**, *155*, 580.

[23] X. Deng, T. Herranz, C. Weis, H. Bluhm, M. Salmeron, *J. Phys. Chem. C* **2008**, *112*, 9668.

[24] C. Kittel, K. Charles, H. Kroemer, K. Herbert, *Thermal Physics*, Macmillan, **1980**.

[25] B. R. Matis, J. S. Burgess, F. A. Bulat, A. L. Friedman, B. H. Houston, J. W. Baldwin, *ACS Nano* **2012**, *6*, 17.

[26] M. Bonmann, A. Vorobiev, J. Stake, O. Engström, *J. Vac. Sci. Technol. B* **2017**, *35*, 01A115.

[27] P. Solís-Fernández, S. Okada, T. Sato, M. Tsuji, H. Ago, *ACS Nano* **2016**, *10*, 2930.

[28] J. H. J. Ostrowski, J. D. Eaves, *J. Phys. Chem. B* **2014**, *118*, 530.

[29] O. Leenaerts, B. Partoens, F. M. Peeters, *Phys. Rev. B* **2008**, *77*, 125416.

[30] T. O. Wehling, A. I. Lichtenstein, M. I. Katsnelson, *Appl. Phys. Lett.* **2008**, *93*, 202110.

TOC

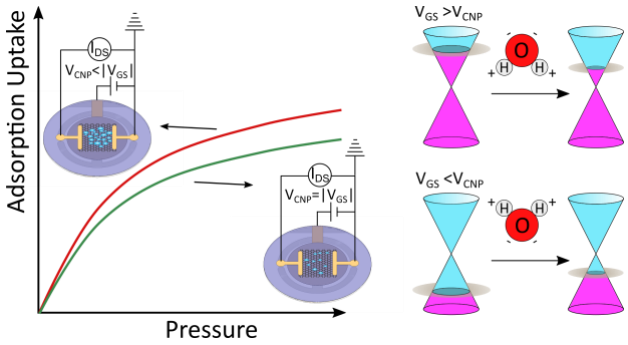
Adsorption Uptake
Pressure
I_{DS}
V_{CNP}<|V_{GS}|
I_{DS}
V_{CNP}=|V_{GS}|
V_{GS} >V_{CNP}
O
H
H
V_{GS} <V_{CNP}
H
H
O

Supporting Information

(a)

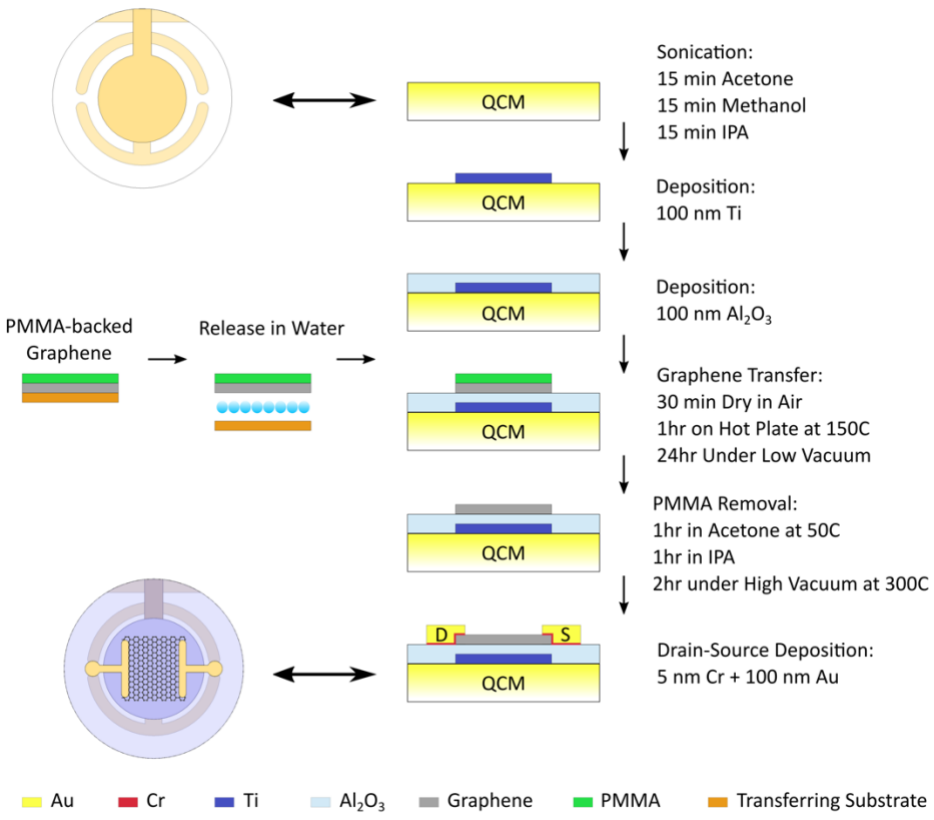

(b)

Figure S1 (a) Schematic of the sample preparation (b) GFET fabricated on a QCM

(a)

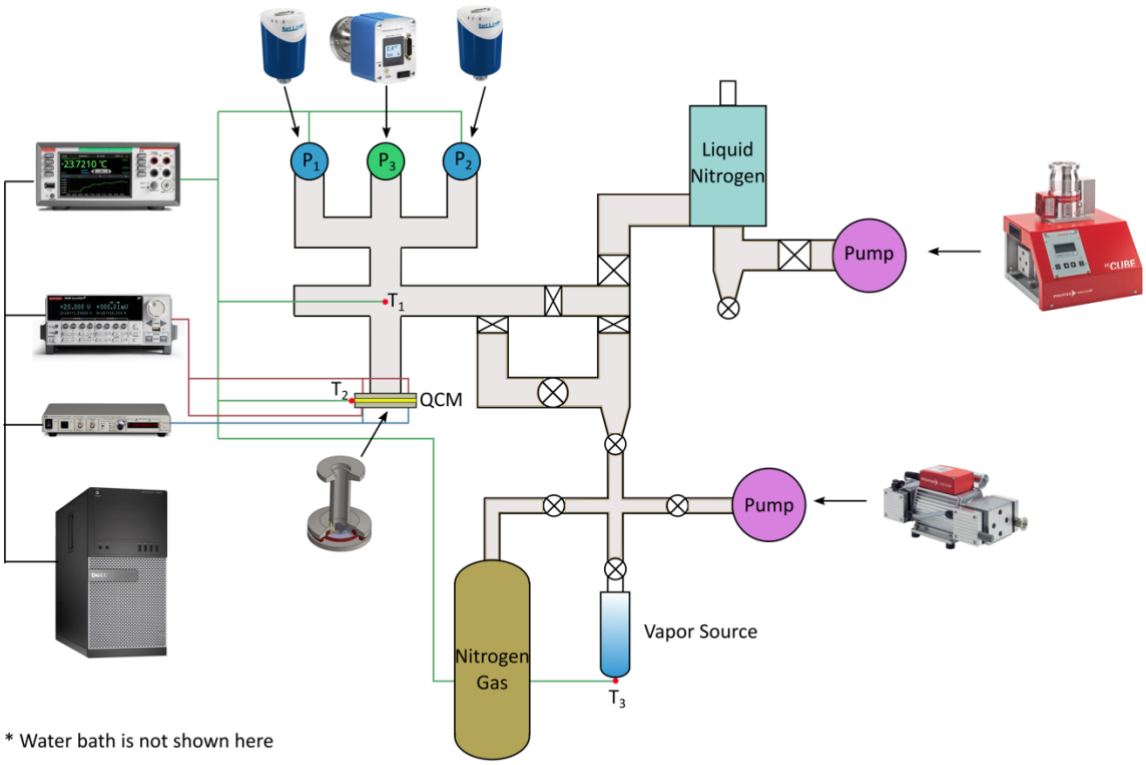

(b)

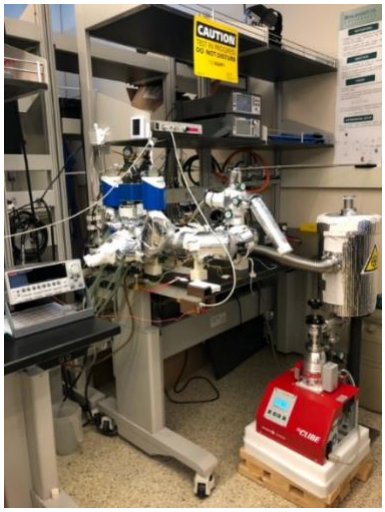

Figure S2 (a) Schematic and (b) the image of the experimental setup

(a) (b)

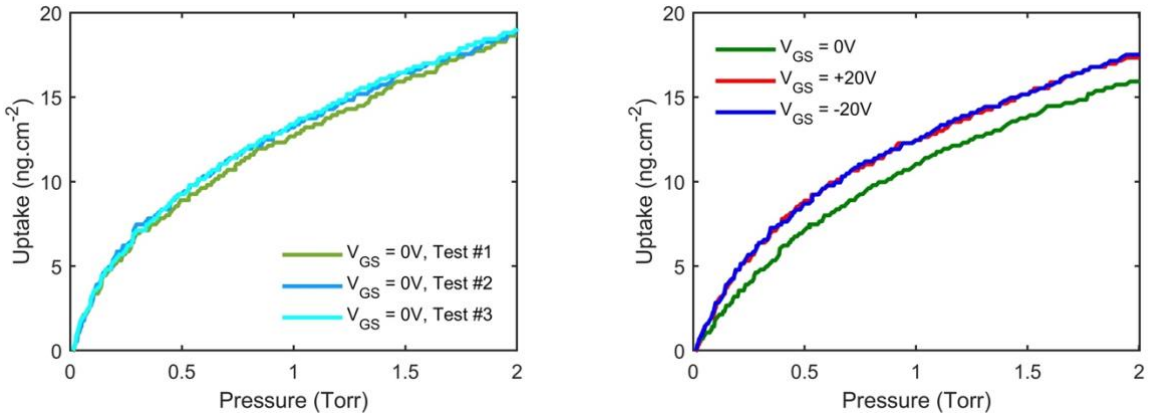

Figure S3 Repeatability of the adsorption Isotherms. (a) Repeatability of the 0V test for the sample with isotherms in Figure 2. (b) The adsorption isotherms for a second sample tested at the three doping conditions

(a)

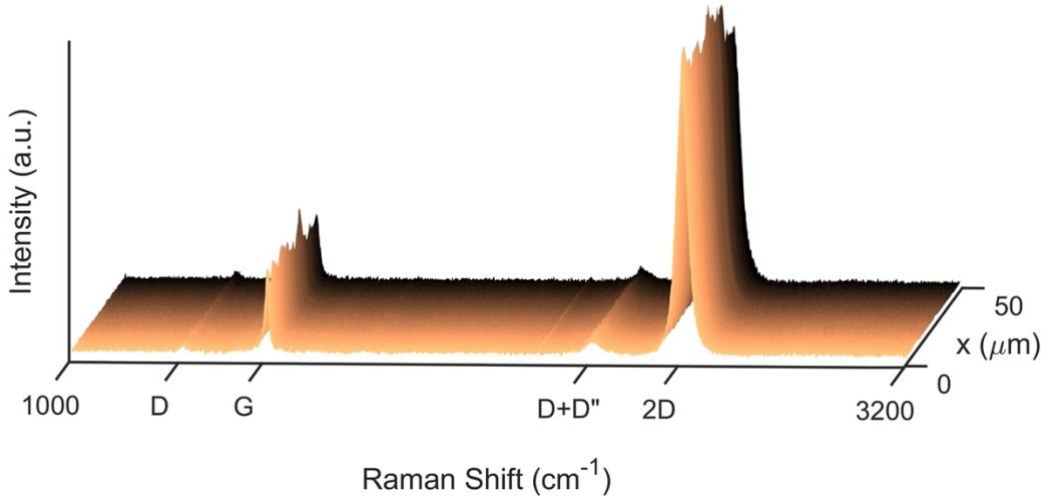

(b)

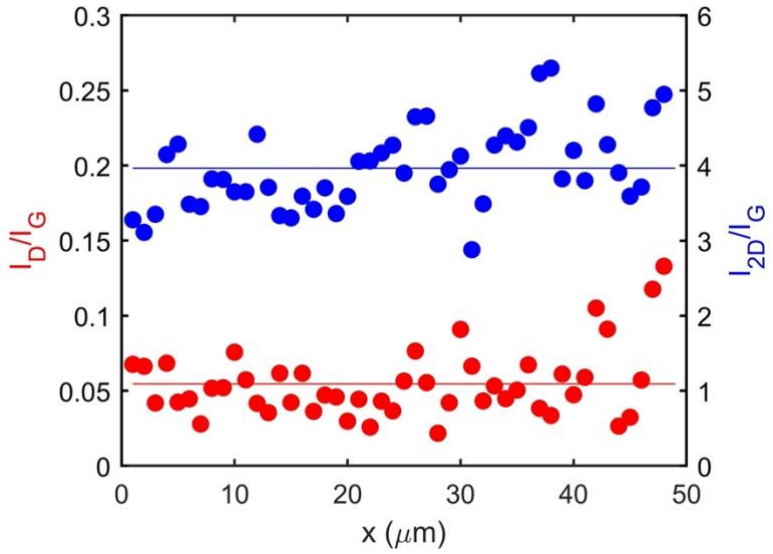

Figure S4 Raman spectroscopy of graphene in a GFET device. (a) The spectra of a random 50 μm line scan. (b) the D to G (left) and 2D to G (right) peak ratios along with their average value (the solid lines). The high 2D to G peak ratio ($I_{2D}/I_G > 2$) shows the presence of a single layer graphene. The small D peak to G peak ratio ($I_D/I_G \sim 0.05$) indicates an insignificant number of defects in the graphene

(a)

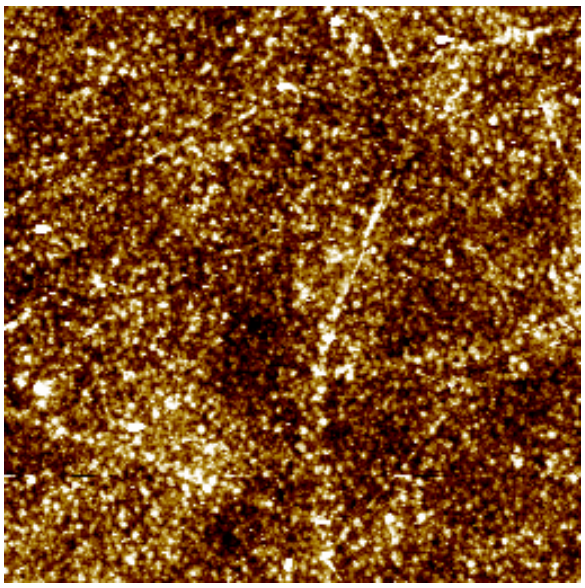

(b)

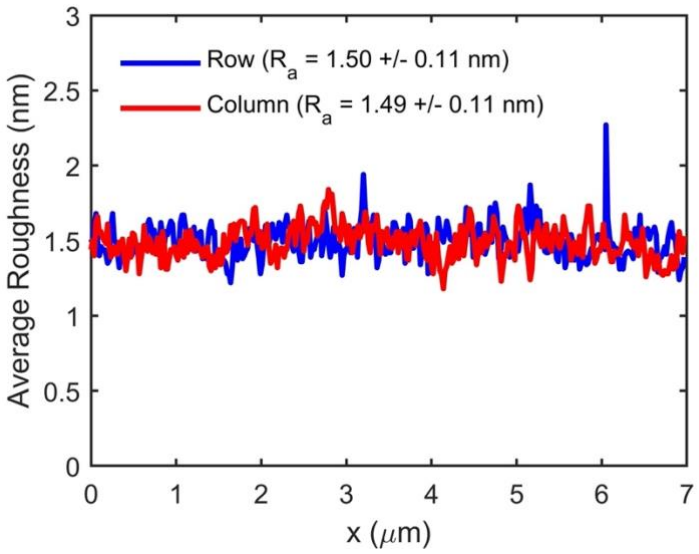

Figure S5 (a) AFM image of a 7 μm by 7 μm scanned area of graphene in a GFET device. (b) The average surface roughness of the scanned area.